JCB

Supplemental material

Risher et al., https://doi.org/10.1083/jcb.201802057

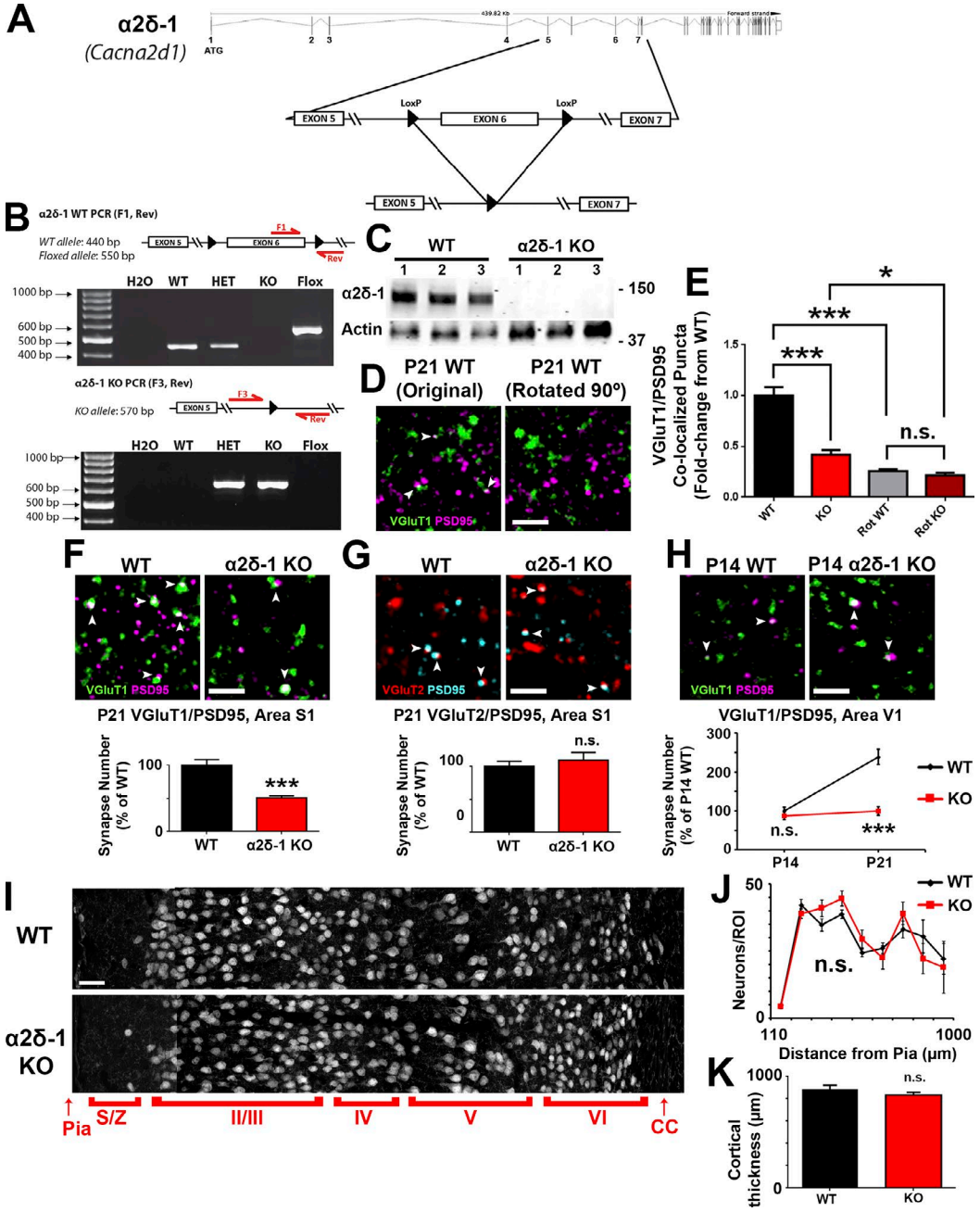

Figure S1. **Design and further verification of α2δ-1–null mouse (related to Fig. 1). (A)** Strategy to silence the *Cacna2δ-1* gene by flanking exon 6 with loxP sites, making it susceptible to excision via Cre recombination. **(B)** Genotyping PCR results for the WT (top), floxed (top), and KO alleles (bottom) of *Cacna2δ-1*. **(C)** Western blot of P21 cortical synaptosome fractions showing α2δ-1 protein expression (top) from P21 WT and α2δ-1 KO brains. Actin (bottom) was used as a loading control. Molecular masses are given in kilodaltons. **(D)** Example IHC images showing the results of synaptic colocalization by chance. For all P21 WT and KO V1 images with VGluT1 (green)/PSD95 (magenta) staining (Fig. 1 D), one channel was rotated 90° with relation to the other channel to create random colocalization (right). Areas of colocalization (white arrowheads) indicate the location of intracortical synapses. **(E)** Quantification shows the results of the rotated images (Rot WT and Rot KO) compared with the original images (WT and KO) displayed as percentages of unrotated WT. *, $P < 0.05$; ***, $P < 0.0001$; one-way ANOVA with Tukey's multiple comparisons post hoc test. **(F)** Top: IHC staining from area S1 showing VGluT1 (green)/PSD95 (magenta) intracortical synapses in P21 WT and α2δ-1 KO ($n = 3$ mice per genotype). Bottom: Quantification of VGluT1/PSD95 synapse number in S1 shown as percentage of WT. ***, $P < 0.0001$; nested ANOVA. **(G)** Top: IHC staining from area S1 showing VGluT2 (red)/PSD95 (cyan) thalamocortical synapses in P21 WT and α2δ-1 KO ($n = 3$ mice per genotype). Bottom: Quantification of VGluT2/PSD95 synapse number in S1 shown as percentage of WT. Nested ANOVA. **(H)** Top: IHC staining from area V1 at P14 showing VGluT1 (green)/PSD95 (magenta) intracortical synapses in WT and α2δ-1 KO. Bars, 2 µm. Bottom: Comparison of VGluT1/PSD95 synapse number between WT and α2δ-1 KO at both P14 and P21 normalized to P14 WT ($n = 3$ mice per age/genotype). ***, $P < 0.0001$; one-way ANOVA with Tukey's multiple comparisons post hoc test. **(I)** IHC confocal images taken at 63× magnification were stitched together to reveal neuronal distribution (marked by NeuN staining) in area V1 between the pial surface (top) and corpus callosum (CC; bottom) from P21 WT and α2δ-1 KO brains. Bar, 50 µm. **(J)** Comparison of P21 WT and α2δ-1 KO for the number of neurons per region of interest (ROI) measured at various distances from the pial surface ($n = 3$ mice/genotype). $P = 0.67011$; one-way ANCOVA. **(K)** Quantification of cortical thickness between P21 WT and α2δ-1 KO V1 ($n = 3$ mice/genotype). Error bars represent SEM. Two-tailed *t* test.

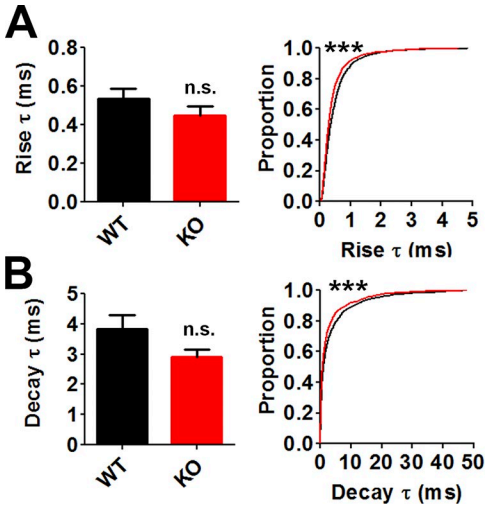

Figure S2. **Faster mEPSC kinetics in α2δ-1 KO neurons (related to Fig. 2). (A)** Rise time of mEPSCs recorded from P21 WT and α2δ-1 KO neurons (*n* = total of 12 cells from three animals/genotype). **(B)** Decay time of mEPSCs recorded from P21 WT and α2δ-1 KO neurons (*n* = total of 12 cells from three animals/genotype). Error bars represent SEM. ***, P < 0.0001; Kolmogorov–Smirnov test.

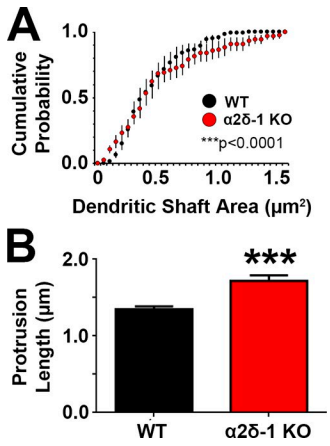

Figure S3. **α2δ-1 KO dendrites have altered morphology (related to Fig. 3). (A)** Cumulative frequency histograms compare dendritic shaft cross-sectional area measurements taken at evenly distributed points along each dendrite (*n* = 10 area measurements/dendrite; four dendrites/animal; three animals per genotype). one-way ANCOVA. **(B)** Comparison of protrusion length between P21 WT and α2δ-1 KO dendrites (*n* = 4 dendrites/animal; three animals per genotype). Error bars represent SEM. ***, P < 0.0001; two-tailed *t* test.

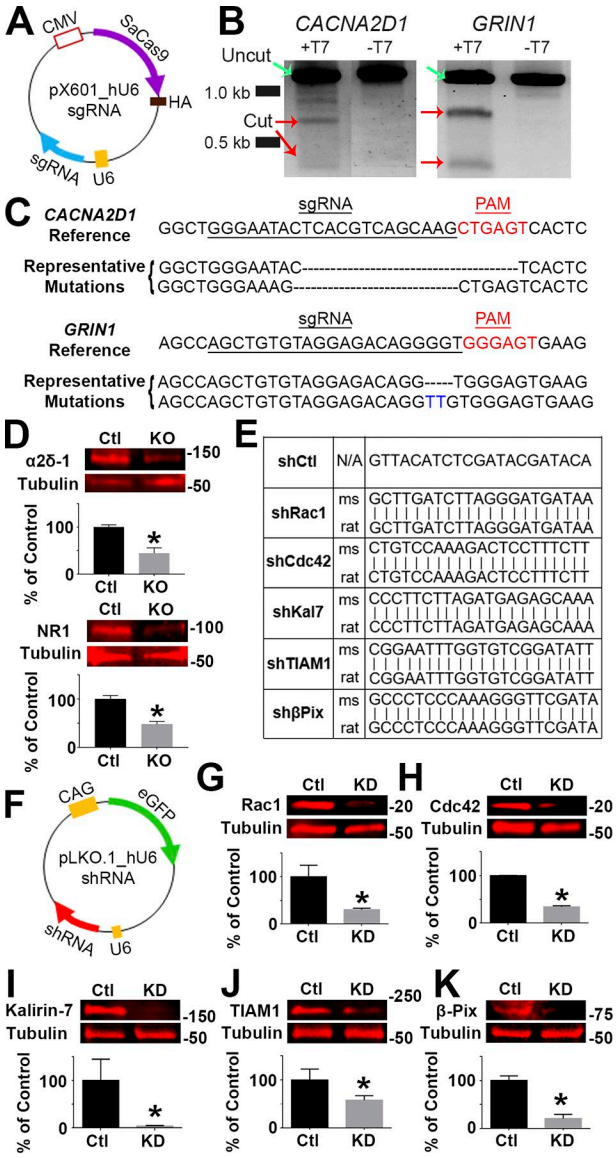

Figure S4. **CRISPR/saCas9 and shRNA gene-manipulation strategies to elucidate the molecular mechanism of TSP-induced synapse formation (related to Fig. 6). (A)** Diagram of the pX601 vector containing an HA-tagged SaCas9 under the CMV promoter and an sgRNA targeting sequence under the U6 promoter. **(B)** T7E1 assay showing presence of cut (red arrows) and uncut (green arrows) DNA after saCas9 transfection of rat lung fibroblasts. No cut bands are seen in the negative T7 controls. **(C)** Example sequencing results showing representative mutations in the *CACNA2D1* and *GRIN1* CRISPR constructs after fibroblast transfection. Underline, sgRNA target site; red text, PAM sequence; dash, deletion; blue text, insertion. **(D)** Top: Western blot of α2δ-1/NR1 expression in rat cortical neurons transduced with pX601 vector virus (Ctl; lacks sgRNA) or sgRNA-containing pX601 virus (KO). β-Tubulin was used as a loading control. Bottom: Quantification of protein levels of α2δ-1/NR1 after saCas9-mediated gene ablation shown as percentages of control (n = 3 replicates per condition from two independent experiments). *, $P < 0.05$; two-tailed t test. **(E)** shRNA targeting sequences of the control construct (shCtl), which does not match the murine genome, and those targeted against Rac1, Cdc42, Kalirin-7, Tiam1, and β-Pix (Cool-1), which each target both the mouse (ms) and rat genome. **(F)** Diagram of the pLKO.1 vector containing an shRNA targeting sequence under the U6 promoter and EGFP under the CAG promoter. **(G)** Top: Western blot of Rac1 expression in astrocytes transduced with pLKO empty vector virus (Ctl) or shRNA-containing virus (knockdown;; KD). β-Tubulin was used as a loading control. Bottom: Quantification of the extent of Rac1 knockdown shown as percentage of control (n = 3 replicates per condition ran twice). *, $P < 0.05$; two-tailed t test. **(H–K)** Same scenario as G except showing knockdown of Cdc42 (H), Kalirin-7 (I), Tiam1 (J), and β-Pix (Cool-1; K) from shRNA-virus transduced astrocytes. Error bars represent SEM. *, $P < 0.05$; two-tailed t test. Molecular masses are given in kilodaltons.

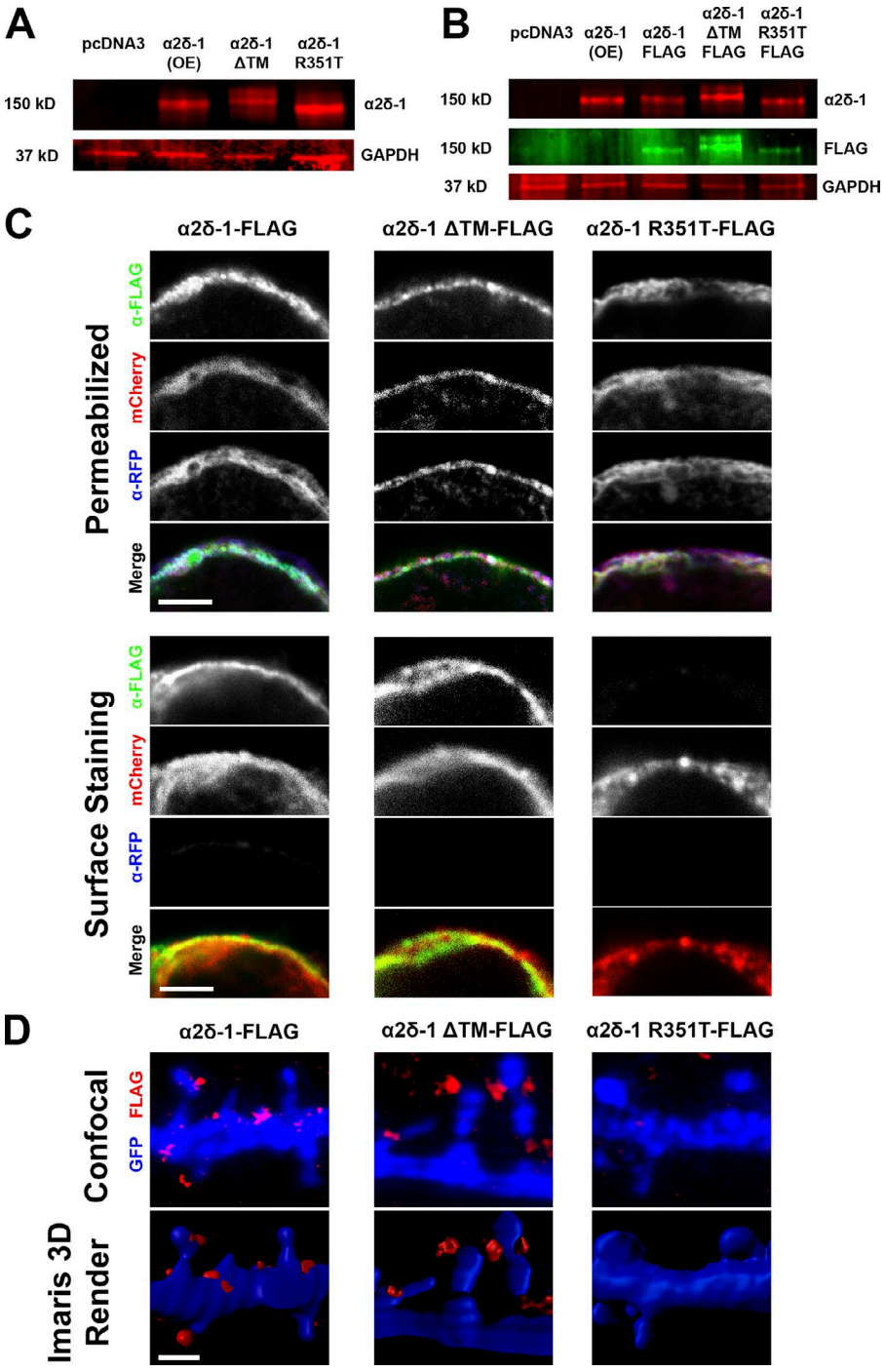

Figure S5. **Cellular expression and localization of α2δ-1 variant constructs (related to Fig. 8). (A)** Western blots showing α2δ-1 expression in HEK293 cells transfected with different α2δ-1 constructs along with a pcDNA3 empty vector as a negative control. **(B)** Western blots showing α2δ-1 and FLAG expression in HEK293 cells transfected with different N-terminal FLAG-tagged and non–FLAG-tagged α2δ-1 constructs along with a pcDNA3 empty vector as a negative control. GAPDH was used as a loading control. OE, overexpression. **(C)** Representative confocal images of HEK293 cells cotransfected with a membrane-targeted mCherry (red) and several different FLAG-tagged (green) α2δ-1 expression constructs. An antibody against RFP (blue) was used to confirm permeabilization in cells treated with detergent (top). Surface staining (bottom) was performed by skipping the permeabilization step before antibody treatment. Bars, 5 µm. **(D)** Representative confocal images (top) and 3D Imaris reconstructions (bottom) of GFP$^+$ cortical dendrites in DEV19 (i.e., P21) rat organotypic slices. Slices were transfected with FLAG-tagged α2δ-1 constructs to visualize protein localization. Bar, 1 µm.